Feedbacks between global supply chain disruption and the spread of SARS-CoV-2

Xingyu Li
University of Michigan
Amin Ghadami
University of Michigan
John Drake
University of Georgia
Pejman Rohani
University of Georgia
Bogdan Epureanu (epureanu@umich.edu)
University of Michigan

Research Article

Keywords: COVID-19, global supply chain, health care resources

Posted Date: March 11th, 2021

DOI: https://doi.org/10.21203/rs.3.rs-279432/v1

Version of Record: A version of this preprint was published at Scientific Reports on July 29th, 2021. See the published version at https://doi.org/10.1038/s41598-021-94619-1.

Feedbacks between global supply chain disruption and the spread of SARS-CoV-2

Xingyu Li[1+], Amin Ghadami[1+], John M. Drake[2,3*], Pejman Rohani[2,3,4*], and Bogdan I. Epureanu[1*]

[1]Department of Mechanical Engineering, University of Michigan, Ann Arbor, USA

[2]Odum School of Ecology, University of Georgia, Athens, USA

[3]Center for the Ecology of Infectious Diseases, University of Georgia, Athens,USA

[4]Department of Infectious Diseases, University of Georgia, Athens, USA

[*]corresponding author, epureanu@umich.edu

[+]these authors contributed equally to this work

ABSTRACT

The pandemic of COVID-19 has become one of the greatest threats to human health, causing severe disruptions in the global supply chain, and compromising health care delivery worldwide. Although government authorities sought to contain the spread of SARS-CoV-2, the virus that causes COVID-19, by restricting travel and in-person activities, failure to deploy time-sensitive strategies in ramping-up of critical resource production exacerbated the outbreak. Here, we analyze the interactive effects of supply chain disruption and infectious disease dynamics using coupled production and disease networks built on global data. We find that time-sensitive containment strategies could be created to balance objectives in pandemic control and economic losses, leading to a spatiotemporal separation of infection peaks that alleviate the societal impact of the disease. A lean resource allocation strategy is discovered that effectively counteracts the positive feedback between transmission and production such that stockpiles of health care resources may be manufactured and distributed to limit future shortage and disease. The study highlights the importance of cross-sectoral coordination and region-wise collaboration to optimally contain a pandemic while accounting for production.

Introduction

SARS-CoV-2, a pathogen that primarily targets the human respiratory system[1], has affected over 200 countries and territories around the world. The disease is responsible for the current global socioeconomic disruptions affecting lives and livelihoods. As of December 5, 2020, there have been 66.7 million confirmed cases increasing with 0.6 million new cases each day. As a result, major enterprises owning more than 12,000 production facilities are shut-down due to quarantine policies, which leads to severe supply chain disruptions[2,3] and a huge dip in international trade, declining between 13% and 32%[4]. Such a disruption in

the supply chain network not only deeply affects the world's economy and health, but also reduces the ability to contain the outbreak. The shortage of critical health care resources due to supply chain disruptions and difficulties in international trade have a significant impact on timely delivery of health care service[5,6].

Since the beginning of the pandemic, efforts have been devoted by local health departments all over the world to ascertain optimal response strategies to mitigate the outbreak. These efforts, however, have been halted by limited critical health care resources at different times and places[7]. The shortage of health care resources originates from surging demands caused by accelerating numbers of COVID-19 cases, misinformation, panic buying, and stockpiling[8]. Resource shortages not only raise health risks but also accelerate the spread of the disease, which exacerbates resource shortages in a vicious circle. With the accelerated spread of the disease, there is a pressing need to sustain the supply chain of critical items to prevent the detrimental feedback between the supply chain disruption and disease growth.

COVID-19 has brought a worst-case scenario affecting critical stock availability: a rapid surge in demand combined with the shortage of substantial raw materials due to global supply chain disruptions[9]. To mitigate resource shortages, simply demanding more critical medical supplies is not enough. In many cases, there are only a few companies that have the expertise to manufacture these products. For instance, sanitizer manufacturing companies in Australia started facing shortages of required raw materials and ingredients soon after increasing their capacity of producing sanitizing gel[9]. Ford's effort of building 50,000 ventilators in July was delayed due to the existing global parts shortages and challenges in scaling up the part productions[10]. Policymakers should not only direct these companies to maximize their production capacities, but also to coordinate other industries into this effort to guarantee material supplies[11].

This pandemic revealed that even high income countries compromised the delivery of health care resources and services as a result of rapid spread and depletion of material stocks. Studies show that the shortage of health care resources in the USA, especially N95 masks, was predictable and preventable with publicly available supply chain data and a careful management strategy[12]. World-wide efforts to mitigate COVID-19 revealed the necessity of an agile and time-sensitive supply chain management strategy during a pandemic, which is difficult to achieve without information transparency regarding the required quantity, rate of use of critical items, and supply chain data across the world[13]. As the virus's global spread escalated, demand for surgical masks has skyrocketed in China starting February. As the largest mask exporting country, China paused its export of face masks[14] and began importing from Europe, Japan, and the United States to alleviate mask shortages[15]. Awareness of such surge demands of critical items has long-term impacts on managerial decisions and disease control. However, the growth of the epidemic creates even more turbulent supply chain and disease situations. It is challenging to foresee intuitively the outcomes from the complex interconnections in order to wisely distribute resources globally.

The need for detailed research considering the dynamic interconnection between managerial decisions, infectious diseases, and shortages of the health care equipment is both important and timely. This study fills this research gap by introducing an integrated model that explicitly captures the positive feedbacks in global supply chain disruption and the pandemic by coupling the network of disease and that of supply chain. Our approach makes effective use of real-world input-output trade data and

ongoing COVID-19 data to improve the fidelity of the model and results. A proactive network control is demonstrated to create an agile and time-sensitive containment strategy, which optimizes worldwide managerial decisions considering predictive impacts on a daily basis. Using a real-world data-based simulation approach, we investigate how different managerial strategies affect the coupled dynamics of the supply chain and disease networks and their evolution. This unique data-driven approach can be used as a stress-test tool to evaluate the robustness and resilience of the supply chain in public health emergencies, which enables a holistic impact analysis of cross-industry coordination and inter-region collaboration to contain an epidemic outbreak.

Coupled model of disease dynamics and supply chain disruption

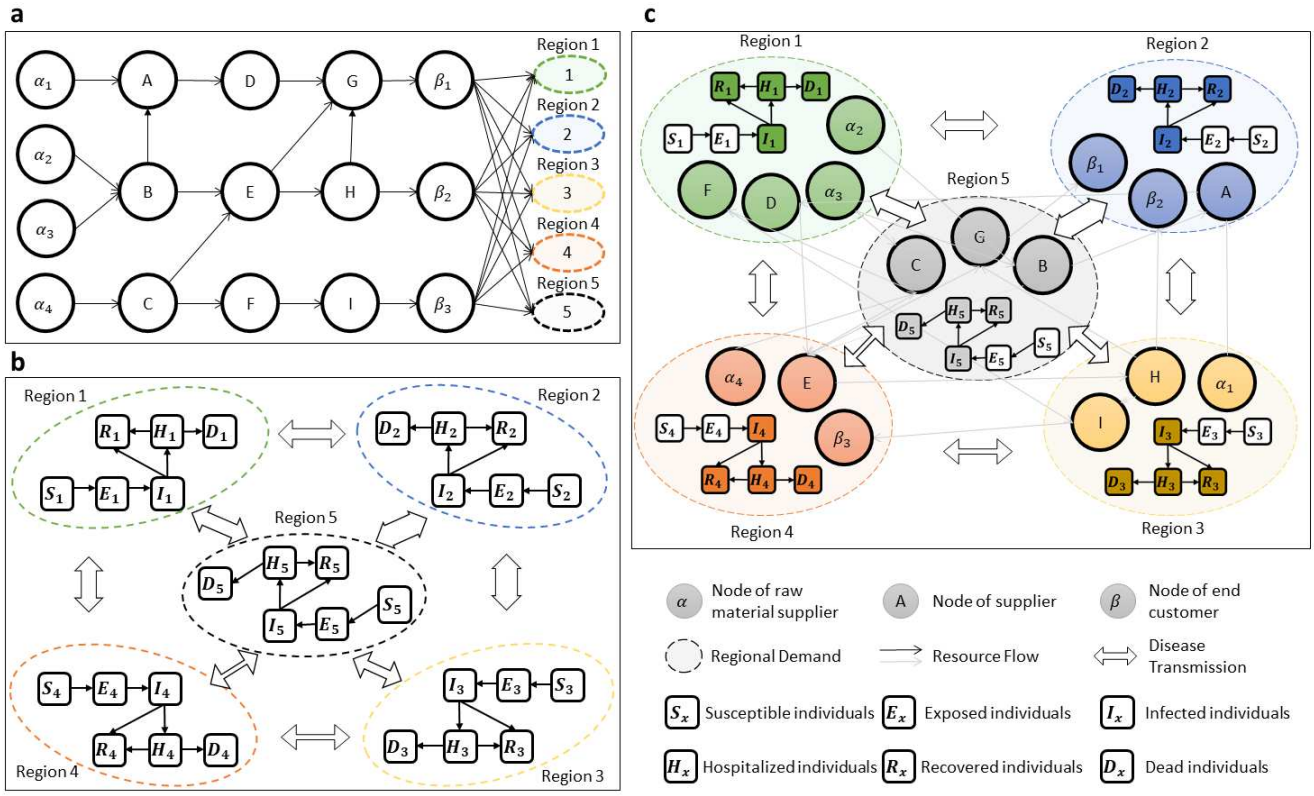

Figure 1. System Model of supply chain and disease dynamic: a) a classic supply chain network with three types of products; **b)** a classic multi-patch disease network for COVID-19; **c)** the coupled networks of multi-patch disease and the production and supply chain.

Model of supply chain disruption in a substantial demand change and quarantine policy

Figure 1a shows a conventional supply chain network including activities, people, entities, information, and resources across diverse industries (Fig. 1a). Under pandemic conditions, suppliers need to coordinate to satisfy regional health care supply needs and face production disruptions. Thus, the regional disease dynamics and geographical location are critical factors in making managerial decisions, i.e., dyed and reorganized nodes that represent suppliers. The pandemic complicates the supply chain configuration and challenges the supply chain management.

Demand for health care resources increased with the growth of the pandemic[16]. For example, masks are critical resources

in medical procedures and also recommended by World Health Organization (WHO) to provide an adequate protection against COVID-19 in public activities[17]. In our model, a disease-dependent demand function explicitly models the surge in medical needs by correlating the demand with the number of infected and hospitalized individuals. In addition, the disease has a substantial impact by disrupting the production capacity for supplies due to quarantined labor force[18] and constrained factory working hour[19]. Studies have found the optimal lockdown policy to be dependent on the prevalence of disease in the local population[20]. We also assume the optimal policy to be adopted, in which case we use a disease-dependent capacity function to connect the production capacity according to the current disease situation is created.

Model of disease dynamics in the severe shortage of medical supplies

Figure 1b shows a multi-patch (metapopulation) compartmental model[21] that represents the kinetics of an epidemic in an idealized susceptible population of connected regions. Studies indicate that the proper usage of face masks can synergetically act together with social distancing to reduce the virus transmission rate[22]. In addition, reliable access to medical supplies and antiviral drug therapy is critical for hospitals to continue to function adequately[13] and to deliver stable and adequate health care[23]. Figure 1c visualizes the connection between shortages of medical supplies, the supply chain, and local disease dynamics, including the transmission rates and recovery rates, which are highlighted in each region.

A shortage-dependent transmission function calculates the transmission rate in each region according to the amount of health care resource shortage per capita. Items like masks and face shields are critical items for preventing COVID-19 as suggested by the WHO[24]. The unsatisfied demands of health care resources impact the ability to adhere to ideal infection control, health worker safety and treatment[25–27] thus changing the transmission of the disease. In COVID-19, special medical devices like ventilators help patients breathe. One ventilator per patient is not possible due to the shortages of ventilators in many countries, which raises the death rate in the population who may likely survive if they receive ventilator support[28,29]. We created a shortage-dependent fatality function that measures the death rate and recovery rate as functions of timely availability of supplies of health care resources.

Results

Considering the geographical separation and economical connections, five regions are selected and connected in a global network to represent the world-wide pandemic outbreak and global supply chain, including Asia, European Union (including United Kingdom), Latin America, North America, and Oceania. We aggregated all suppliers that produce goods and services in each region, and considered the capability of trading among regions. Three data sets are used for estimating the parameters of the coupled model of supply chain and disease networks, which is formulated to represent the positive feedbacks of supply chain disruption and disease growth. In the disease network, the transmission rate is estimated on a daily basis by fitting the pandemic data reported by Johns Hopkins University Center[30]. Tourism data provided by the World Tourism Organization[31] and international air travels history reported by the International Air Transport Association (IATA) are aggregated to approximate the connectivity among regions. A global supply chain network is built from the Global Trade Analysis Project (GTAP) database (version 10)[32]. Industries are grouped up into 10 sectors defined by GTAP. The human health and social work (HHS)

sector are separated as a special sector to represent the expenditure on health care resources in human health and social work[33]. The resources required by HHS are considered to correlate with the emergence of COVID-19[34], reflecting the surge in demands of critical medical supplies. Assuming each regional sector as a producer, the following information is obtained for each regional sector: (1) the bill of material in production, (2) the pre-pandemic production capacity, and (3) the cross-regional resource flow at equilibrium.

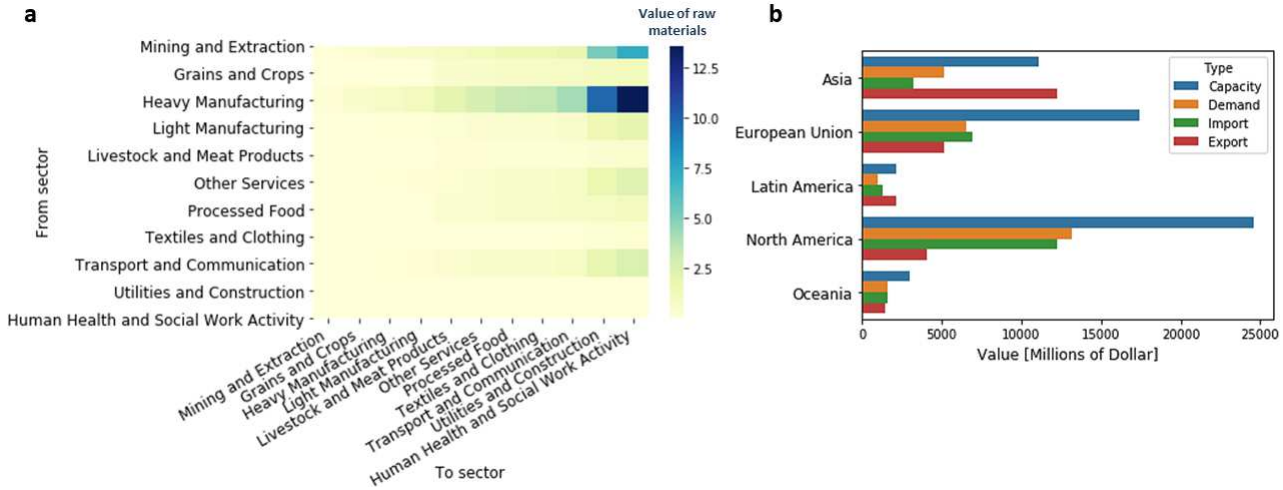

Figure 2. Global trade data analysis based on GTAP 10: a) Values of required raw material from different sectors to satisfy the doubled production of each sector. The rows of the table define sectors to provide the raw materials, and the columns of the table define sectors which double their production. **b)** Comparison of the production capacity, demands, and trade at the equilibrium between different regions. Here, the capacity is calculated by the total yearly production estimated from the total export and self-consumed resources. Demands are estimated based on the resource consumption from the household and government. Trade history is calculated based on resources exchanges in each region, including household, government, and companies.

Figure 2a lists all sectors used in this study, and compares the demand inputs from other sectors if productions of each sector were to double. The increasing HHS production depends on inputs from many other sectors. The major inputs are from heavy manufacturing, mining, and extraction. Light manufacturing, other services, and transport and communication are dependent sectors also. A strong dependence emphasizes the need for sectoral coordination to ensure sufficient material supplies are available to increase the production of health care resources. Figure 2b shows the diversity of production and demand among regions, in terms of capacity, demand, and trade at equilibrium measured in millions of dollars. North America has the highest HHS capacity, import, and demand, followed by the European Union. Latin America and Oceania have low production capacity and low needs for HHS resources. Asia is a major export region. The regional diversity highlights the need for analyzing the risks of regional production disruptions, as well as the customization of the containment strategy for each region.

Cross-Sector Coordination

We study the positive feedback of disease dynamics and supply chain disruption in a 100-day discrete-time simulation model initialized by the global COVID-19 data on March 1st. Managerial decisions are updated daily by a proactive control of the supply chain network with consideration of production and inventory constraints. The coupled system of two networks

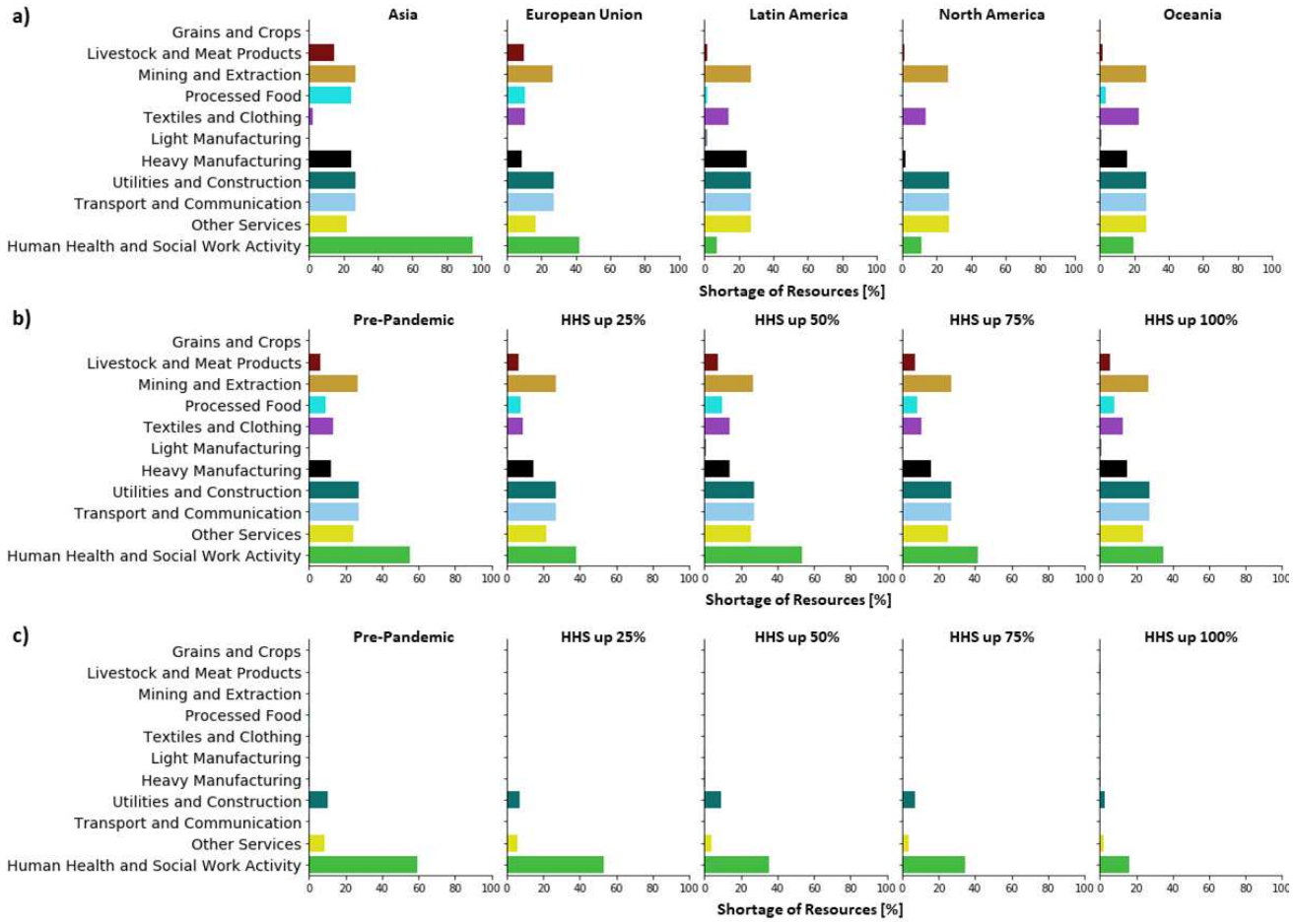

Figure 3. Sectoral impacts of increased HHS capacity: a) Without coordinating other sectors, the regional shortage of resources after doubling the production of HHS in each region. **b)** Without coordinating other sectors, the averaged shortage of resource in five ramp-up scenarios, in terms of the pre-pandemic capacity (100), ramp-up by 25% (125), ramp-up by 50% (150), ramp-up by 75% (175) and , ramp-up by 100% (200). **c)** With coordinated supply chains, the averaged shortage of resource in five production ramp-up scenarios.

enables the control to weigh multi-objectives in the disease control and economic losses, thus finding a balanced solution. With a higher capacity of producing HHS resources, the containment strategy tends to raise the HHS production to alleviate the shortage of HHS resources so as to reduce the spread of the disease. Figure 3a shows the results of a stress test to identify the vulnerable sectors in satisfying the demands from a health emergency. Results show that Grains and Crops is the least impacted sector among all countries due to its weak dependence on other sectors. Transport and Communication is the bottleneck sector that limits further increase of HHS production. Because the differences in regional capacities, sectoral impacts also vary. Asia and Oceania are impacted the most in their Heavy Manufacturing sector. Interestingly, the analysis shows that the shortage of Processed Food, and Livestock and Meat Products in Asia are significantly greater compared to other regions, which is consistent with the raise in the price of pork reported in Asian countries[35,36].

Figure 3b shows the shortages for four different HHS ramping-up scenarios. Despite the forced increase in capacity by the policy-maker, the capacity is dynamically updated according to the evolving disease situation by the disease-dependent

capacity function. With increasing production capacity, the shortage of HHS does not reduce monotonically, but fluctuates around 40%. As a result, significant shortages are observed in other sectors, including Mining and Extraction, Transport and Communication, and Utilities and Construction, which overlap with dependent sectors in the Figure 2a. Other sectors, such as Textiles and Clothing, suffer a remarkable shortage due to the shared input materials with the HHS resources, i.e., cloth and masks. Increase in the production capacity is not enough to meet the surge in demands due to the limitations of raw materials. Without coordinated sectors, the ramp-up of production capacity incurs the overuse of materials in the existing stockpiles, which leads to further raw material shortage in the future operation, thus deepening the disruptions in producing HHS resources.

Figure 3c shows the sectoral impacts when sectors are coordinated, namely, all the other sectors are able to provide sufficient raw materials for HHS production. With increasing HHS production capacity, a clear decreasing trend of the HHS shortage is observed, reducing from 60% shortage to less than 20% shortage. Note that even with sufficient production capacity, shortages exist in Other Services and Utility and Construction, which require raw materials from the HHS resources for production.

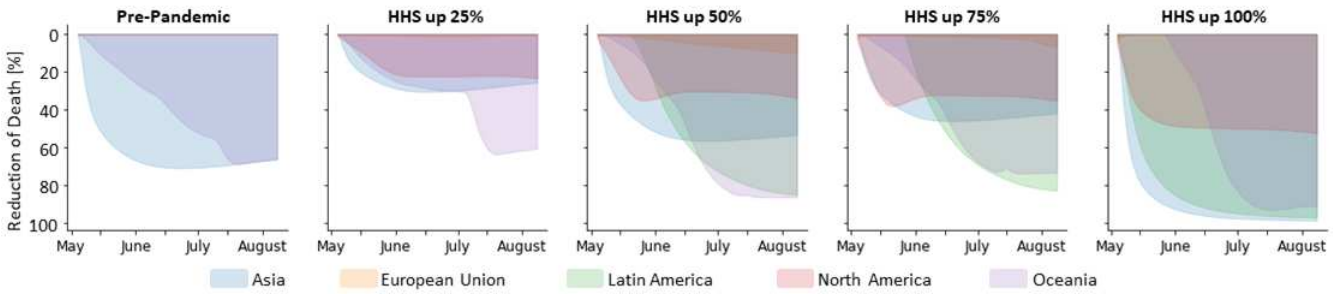

Figure 4. Disease impacts for increased HHS capacity. Assuming coordination of the supply chain is possible, the diagrams show the perentage of fatality reduction in different regions with the increasing production capacity of HHS resources, in terms of the pre-pandemic capacity (100), ramp-up by 25% (125), ramp-up by 50% (150), ramp-up by 75% (175) and , ramp-up by 100% (200). The fatalities simulated in the pre-pandemic capacities is used as a benchmark to calculate the reduction percentage.

Figure 4 shows the influence of improved HHS production on the disease outcomes. As a benchmark, the number of dead is calculated based on simulation results according to the pre-epidemic production capacity. The percentage of reduction is calculated by comparing the total number of fatalities to the benchmark at each time instance. With coordinated supply chains, an increase in HHS capacity at the early stage of the pandemic substantially reduces the number of fatalities as well as the duration of the outbreak. In the coupled model, a reduction in HHS shortage reduces the disease transmission rate, thus suppressing the number of newly added infections due to better personal protection. In addition, the fatality rate decreases with more medical resupplies that reduce the fatality rate. As a result, the number of fatalities is reduced by 90% by doubling the capacity of HHS in March.

Lean Resource Management and Regional Collaboration. We sought to confirm that key improvements are possible in lean management of HHS resources and regional collaboration by exploring the managerial decisions made by network proactive control. In this study, the analysis starts from March 1st based on COVID-19 data, and the system evolves for 30 days based on the pre-epidemic supply chain managerial strategies. Then, a 100-day simulation is conducted based on three containment

strategies: 1) pre-epidemic equilibrium (PE) strategy: adopt the pre-pandemic managerial decisions; 2) supply chain network optimization (SCO) strategy: optimize the managerial decisions based on the demands and inventories; 3) coupled network optimization (CNO) strategy: optimize the managerial decisions based on the interactions in the coupled networks. Figure 5 shows the effectiveness of these containment strategies in terms of infections in different regions.

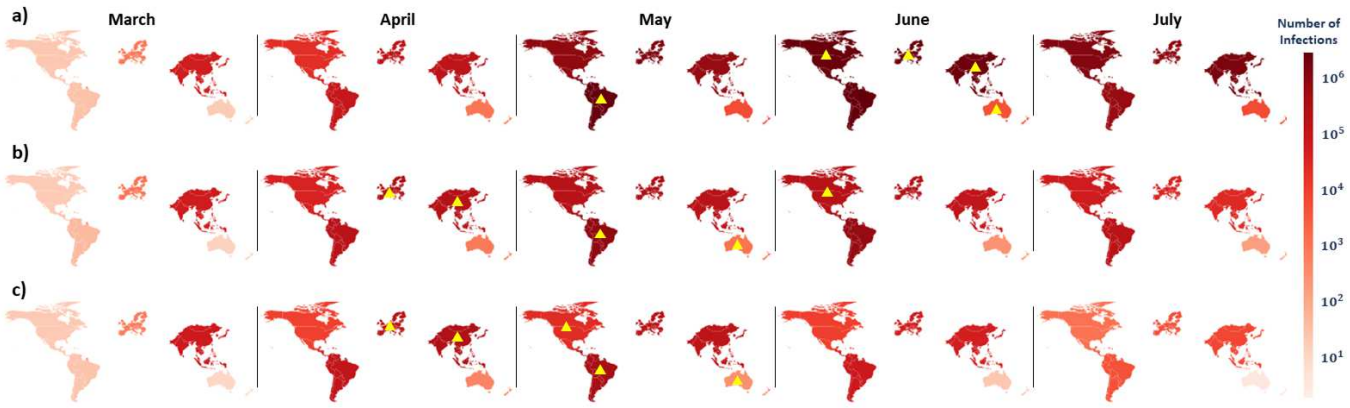

Figure 5. Impacts of strategies on infections: a) The evolving infections under the pre-pandemic containment strategy. **b)** The evolving infections for the SCO strategy. **c)** The evolving infections for the CNO strategy. The darkness of each region represents the number of infections. The yellow triangle marks the occurrence of the peak of infection.

Figure 5a shows the number of infections in the PE strategy which skyrockets in the three months following March. The peak values of the 4 regions including Asia, European Union, North America, and Latin America occur simultaneously around July 1^{st}, leading to extremely high demands for critical medical supplies and severe global production disruptions, which poses extreme challenges in the pandemic containment. Figure 5b shows the simulation results for the SCO strategy. The number of infections is notably reduced due to the dynamic supply chain transformation achieved by network proactive control. Figure 5c shows simulation results for the CNO strategy. The production and supply chain decisions are made with consideration of the positive feedback between the production disruption and pandemic growth. The number of infections is reduced further and the pandemic almost fades in July. Note that the peaks of regional infections are staggered in both SCO and CNO strategies. Both these optimization-based containment strategies lead to a spatiotemporal separation of infection peaks to split the demand load. Moreover, these containment strategies also ensure that at least one of the major HHS providers is available to support other regions in each period of time, thus preventing an intense growth of the disease.

Figure 6a summarizes the loss of production capacity of each region in the SCO strategy. Without considering the positive feedback, North America and European Union suffer capacity losses in May (15.75% and 19.33%) and June (16.57% and 13.44%). As a comparison, the production disruptions for European Union and North America are reduced to 2.11% and 12.15% in May and 0.9% and 3.86% in June respectively in the CNO strategy (Fig. 6b). The better recovery of production capacity results in more HHS resources that can be produced and distributed to other regions for disease control, thus leading to a quick production recovery, especially for the regions with stronger industrial capabilities. Note that Latin America suffers a higher production disruption compared to other regions. The lack of capacity of HHS production makes Latin America unable

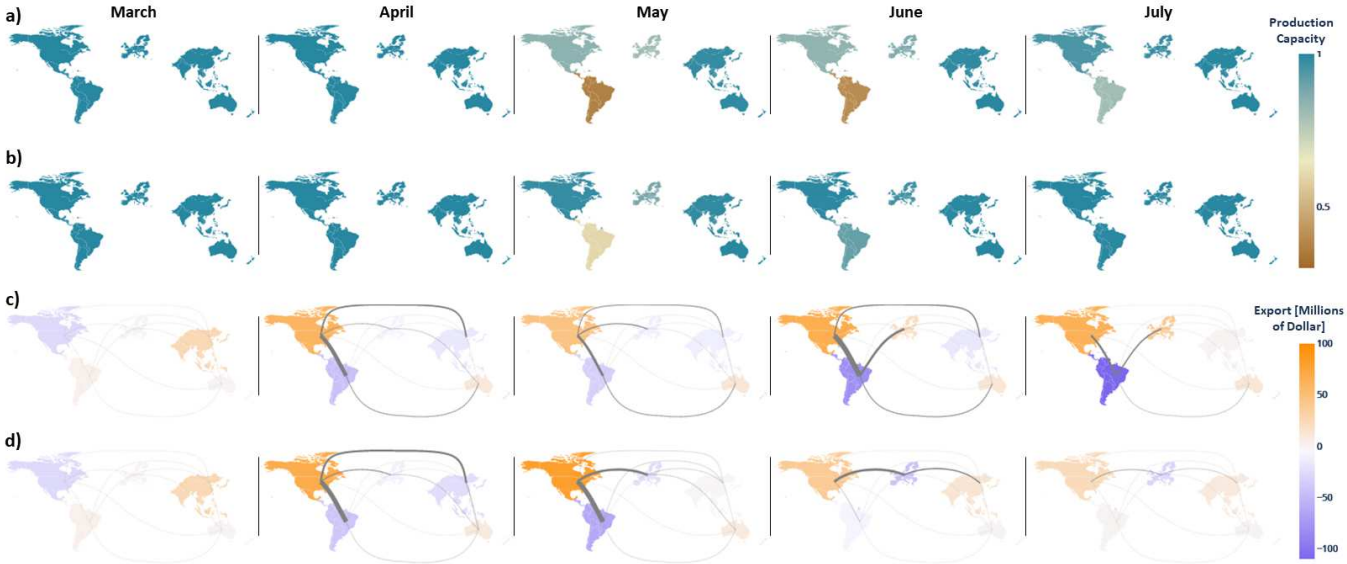

Figure 6. Production disruption and trade decisions of different containment strategies: a) The dynamics of available production capacity by region in the SCO strategy. The color bar represents the percentage of available production capacity of each region. **b)** The dynamics of available production capacity in the CNO scenario. **c)** The total import and export decisions of each month in the SCO strategy; The strength of connections of regions marked by the width of the corresponding lines. **d)** The total import and export decisions of each month in the CNO strategy; the strength of connections of regions marked by the width of the corresponding lines.

to satisfy the surge in HHS demands under a health emergency, which highlights the need for inter-regional collaboration.

Figure 6c,d show the trade history of the world's supply chain corresponding to the SCO and CNO strategies, respectively. The results in March are a benchmark for the inter-region collaboration simulated in the pre-pandemic strategy. Much stronger collaboration among regions is observed after April when the network proactive control starts. Although Oceania and Latin America both lack the capacity to produce HHS resources, infections in Oceania are delayed, which reserves the production capacity in health care resource preparation ahead of time to contain the disease growth. In contrast, low capacity and high existing infections make Latin America rely on imports from other regions for disease control. The comparison shows that the managerial decisions depend on regional production capacity as well as the connectivity to other regions.

Although both containment strategies suggest similar managerial decisions in April, the SCO containment strategy does not account for the positive feedback, and thus inaccurately forecasts the changes in disease trends from historical medical supplies data. Due to the positive feedback, a small difference in predictions may evolve into a distinct outcome for the disease. By considering the positive feedback, Asia and European Union receive 50% and 42% more HHS supplies from North America and Oceania in the CNO strategy. Although the importance of additional supplies might not be immediately recognised, it makes a significant long-term impact on containing the disease if applied at the early stages of the pandemic. For example, Asia is the import region in the first two months. The increased imports in April and May slow down the pandemic growth. The improvement in the disease dynamics shortens production disruptions and reduces the demand from infected individuals and hospitals. As a result, Asia changes to an export region in June. The model predicts that the disease is significantly reduced in

Latin America by the inter-region collaboration although that is the region hardest hit by the disease. The lower amount of infections in turn reduce imported infections to the other regions, and that slows the spread of the disease.

In the SCN strategy, Asia needs to import HHS resources from other regions all the time. Due to the limited health care resources, the pandemic in Latin America starts to grow and requires more urgent medical aid from other regions, thus resulting in a totally different pandemic situation as shown in Fig. 5. In July, Latin America still needs to order health care resources to satisfy HHS demands from other regions, while these other regions start to export health care resources during the active pandemic (e.g., export from European Union). The consideration of the positive feedback and the transparency of data regarding supplies enhances the CNO containment strategy, leading to a lean management of HHS resources to better control the growth in HHS demands and to limit the disease spread.

Discussion

Until now, research has focused on the economic impact of public health interventions[37,38] or on improving the accuracy of disease prediction[39,40] to address the challenges posed by COVID-19. Yet, many efforts have failed to account for the correlations between the pandemic growth and supply chain disruption. Supply disruption not only slows down governments' ability to respond, but also allows the disease to spread by limiting resources, which in turn increases demand. Our model views the pandemic growth and supply chain disruption as mutually reinforcing pressures, resulting in an increased lack of HHS resources that deepens the supply chain disruption and the damage to public health. In our work, the interconnected supply chain and pandemic networks are connected to analyze the mutual influence in HHS resource shortages, disease dynamics, and production disruption. Network proactive control algorithms can provide agile and time sensitive containment strategies that control the disease by improving the supply chain managerial decisions to ensure availability of HHS resources while considering the trade-off between disease growth and economic losses.

Our discovery based on real-world data uses the status quo as benchmark to highlight the effectiveness of different containment strategies in what-if scenarios. The existing diversity in economy and public health status in different regions of the world are modelled to address the need for customization of disease containment and inter-region collaboration strategies. The significance of our analysis may be observed by contrasting the results of Fig. 5 reflecting different outcomes for the pandemic depending on the selected strategies. Foreseeing the positive feedback between supply chains and disease dynamics enhances our understanding of the future of the pandemic and supply chain disruption, leading to an agile and lean resource allocation strategy that effectively decelerates the spread of the disease and facilitates production recovery.

The shortage of key equipment and materials during the COVID-19 pandemic and meeting the surging demands of medical and personal protective equipment has been a significant challenge since the beginning of the pandemic. Researchers acknowledge that ramping-up HHS resource production may not be as simple as raising the production capacity, but requires the coordination of raw materials[9,11]. In addition, the recent surge in HHS demands was found to stress supply chain networks and deepen disruptions[3,41]. Here, the proposed model has not only provided quantitative analysis of material shortage required

to meet the demands to ramp-up HHS production, but also measured the minimal sector impacts with managerial decisions that trade off the human cost and economic losses. Although these discoveries do not reflect all the underlying causes of supply chain disruption, they significantly advance our ability to manage the situation by informing decision makers about vulnerable sectors that have to be coordinated during an outbreak.

Given the increased HHS production, enhanced inter-region collaborations at the start of the pandemic would have shortened the pandemic period and reduced the threat to public health. In our model, containment strategies are customized by regions according to their industrial structure and production capacity, thus leading to distinct roles of regions in a health emergency. Results highlight the need to strategically distribute the HHS stockpiles differently by region in order to prevent future resource shortages. The active control model of the supply chain network tends to distribute resources to regions with major HHS production capacity to prevent those regions from being disrupted by the lockdown policies caused by the pandemic, thus improving the long-term HHS production supplies.

Comparing the results of the CNO and SCO strategies, the impact of the positive feedback of disease dynamics and supply chain management was highlighted. The subtle difference due to ignoring the positive feedback in predicting the disease dynamics and the HHS demands resulted in small strategic shifts. These subtle shifts in the early stages of the pandemic led to a substantial divergence in the long-term managerial strategies due to the feedback between the disease dyanmics and the supply chain disruption. In the SCO strategy, ignoring the positive feedbacks makes the HHS export countries to overestimate HHS demands thus being conservative in exporting, which in turn reduces the amount of HHS resources other regions receive. The increase in HHS shortages accelerate the disease growth, which in turns demands more HHS in the future, leading to a butterfly effect[42], where a small change in managerial decisions for a coupled nonlinear system can result in large differences in outcomes.

In summary, we proposed a coupled disease and supply chain network model using real-world data, and adopted existing prevention policies. We quantitatively assessed the impacts of cross-sectoral coordination and agility in containing the outbreak. We explored different containment strategies for critical medical supplies to seek the best managerial outcome in terms of minimizing both the number of fatalities as well as the losses in meeting demands. In our model, managerial decisions are customized based on the ability of different world regions to produce required resources and the risk of infection in terms of transmission rate. Such customized decisions could lead to time-sensitive strategies, illustrating the importance of agility in prediction, lean resource management, and collaboration in pandemic control and economic recovery. Results of this study highlight the importance of cross-sectoral coordination and information transparency between suppliers across the world to contain a pandemic.

Methods

Coupled supply chain and disease network. Each region is modeled as a patch with a disease model for simulating the disease dynamics and a production-inventory model for production scheduling and planning. In particular, we use an SEIRHD

model of the disease with six compartments [43], including susceptible (S) reflecting the part of the population that could be potentially subjected to the infection, exposed (E) representing the fraction of the population that has been infected but is not infective yet, infected (I) representing the infective population after the latent period, hospitalized (H) representing the fraction of infected individuals who need hospitalization, recovered (R) representing the population that has successfully cleared the infection, and the fatalities due to the disease (D). The production and inventory model of region i is described by two states at each time t: 1) inventory level of type k resource, $V_{i,k}(t)$; 2) backlogged demands for the type k resource, $U_{i,k}(t)$. We denote the resource of type h as HHS resources. Thus, $V_{i,h}(t), U_{i,h}(t)$ are the inventory level and demand for the HHS resources in region i. Regional managerial decisions in region i, including production of type k resource, $w_{i,k}(t)$ and distribution to the public $o_{i,h}(t)$, are the decisions to be optimized in the local inventory production planning. The resource production follows the bill of materials $M_{k',k}$, which specifies the amount of type k' resource required to product a type k resource.

To model connectivity in the system and the contact between regions, the infection in region i is affected by the number of infected individuals in other regions (due to interrelations such as travel), which creates a multi-patch disease network. We use $\beta_{i,j}$ as the rate at which susceptibles in region i are infected by infected individuals from region j. We assume that the infection can be passed between any pair of regions, albeit possibly via intermediate regions. We assume that $\beta_{i,j} \ll \beta_i$ to reflect the fact that the between-patch transmission parameters are significantly smaller compared to the within-patch transmission parameters. Cross-region trade and supplies connect the regional inventories as a global production and supply chain network involving region-wise trade decisions, i.e. $o_h^{i',i}(t)$ for importing resouces of type k from region i' to i. Summarizing the above description, we model the dynamics of the disease in region i using the following set of equations:

$$
\begin{aligned}
S_i(t+1) &= S_i(t) - S_i(t)\sum_j \frac{\beta_{i,j}(t) I_j(t)}{N_j} && (1)\\
E_i(t+1) &= E_i(t) + S_i(t)\sum_j \frac{\beta_{i,j}(t) I_j(t)}{N_j} - \gamma_{EI} E_i(t) && (2)\\
I_i(t+1) &= I_i(t) + \gamma_{EI} E_i(t) - (\gamma_{IH} + \gamma_{IR}) I_i(t) && (3)\\
H_i(t+1) &= H_i(t) + \gamma_{IH} I_i(t) - (\gamma_{HR} + \gamma_{HD}) H_i(t) && (4)\\
R_i(t+1) &= R_i(t) + \gamma_{IR} I_i(t) + \gamma_{HR} H_i(t) && (5)\\
D_i(t+1) &= D_i(t) + \gamma_{HD} H_i(t) && (6)\\
V_{i,k}(t+1) &= V_{i,k}(t) + \sum_{i'} o_{i',i,k}(t) - o_{i,i',k}(t) - \sum_{k'} M_{k',k} w_{i,k'}(t) + w_{i,k}(t) - o_{i,k}(t) && (7)\\
U_{i,k}(t+1) &= U_{i,k}(t) + \delta U_{i,k} - o_{i,k}(t) && (8)
\end{aligned}
$$

where, N_i is the size of population of region i. We note that $\gamma_{IH} = \delta_H/\tau_I, \gamma_{IR} = (1-\delta_H)/\tau_I$, $\gamma_{HD} = \delta_D/\tau_H$, and $\gamma_{HR} = (1-\delta_D)/\tau_H$, where c reflects the percentage of infected individuals hospitalized, and δ_D reflects the fatality rate. τ_I and τ_H represent the average infectious period and average hospital stay in days, respectively. In our analysis, we choose $\gamma_{EI} = 1/5.2$ days, $\tau_I = 4.6$ days, and $\tau_H = 10$ days according to values reported in previous studies [44]. We fit the model to data of COVID-19

to find the coefficients δ_{Di}, δ_{Hi} and $\beta_{i,j}$ at each time instant. The proposed modeling framework allows for different types, intensities, and duration of interventions to be implemented in each region, and thereby illustrates how these interventions impact the disease dynamics and resulting number of infections and fatalities through time. In particular, we consider Non-pharmaceutical Interventions (e.g., social distancing) and the shortage of HHS resources for a set duration applied as a scaling of the transmission rates for all infected individuals.

Coupling Functions

Disease-dependent capacity function Studies have confirmed the dependence of optimal lockdown policy on the disease fraction in the population[20], which links the pandemic severity to the production capacity. Assuming that the optimal lockdown policy is adopted, the production becomes a function of the existing disease situation, i.e., the percentage of infected and hospitalized. These simplifications allow us to describe a real-time evolving supply chain network, together with the disease spreading on it, to describe the expected amount of production capacity available during the pandemic, namely

$$w_{i,k}(t) \leq W_{i,k} = e^{-\gamma_w \frac{I_i(t)}{N_i}} \bar{W}_{i,k}, \tag{9}$$

where $\bar{W}_{i,k}$ is the pre-pandemic production capacity and γ_w is a scaling parameter designed such that only 1% production capacity remains available when the percentage of active infections reaches 1% of the total population.

Disease-dependent demand function There is a broad range of estimates of critical medical supplies required to care for COVID-19 patients, which vary depending on the number, speed, and severity of infections[11,16,45]. Thus, we created a function to characterize how governments and households issue orders to their suppliers under the pandemic. Demands are separated into commercial resources, $\delta U_{i,k}, \forall k \neq h$ and HHS resources, $\delta U_{i,h}$. Additional HHS resources are considered to be dependent on the severity of the pandemic and correlated to the number of existing infected individuals $I_i(t)$ and hospitalized individuals $H_i(t)$. The product demands of other sectors remain the same as pre-pandemic, namely

$$\delta U_{i,h} = \gamma_I I_i(t) + \gamma_H H_i(t) + a_{i,h}(t) \tag{10}$$

$$\delta U_{i,k} = a_{i,k}(t), \qquad \forall k \neq h \tag{11}$$

where γ_I and γ_H measure the expenditures needed to treat a susceptible individual and an infected individual on a daily basis (we assume $\gamma_I = 0.0001, \gamma_H = 0.002$), which are roughly estimated based on the direct medical costs of MERS coronavirus[?]. $a_{i,k}(t)$ is the daily consumption of resources of type k during the pre-pandemic period.

Shortage-dependent transmission function To model the transmission rate, we consider three elements for each region i, including a base transmission rate $\beta_0^i(t)$ representing the transmission rate without any non-pharmaceutical interventions (NPI) measures, a health care coefficient $c_{H,i}(t)$ representing reduction in the transmission rate due to proper usage of HHS resources, and an NPI coefficient $c_{N,i}(t)$ representing the reduction in contact rate due to change in economic activity and NPI such as social distancing and curfew. We define $c_{H,i}(t) = 1 - \frac{2(1-P_l)}{1+e^{\frac{10^6 U_{i,h}(t)}{N_j}}}$, where P_l is the minimum protection measure with zero health

care stocks ($P_l = 0.5$, reflecting 50% effectiveness of HHS products if used properly[46,47]). Based on these coefficients, the disease transition rate $\beta_i(t)$ of region i is expressed as

$$\beta_i(t) = \beta_{i,0}(t)c_{N,i}(t)c_{H,i}(t) \tag{12}$$

Shortage-dependent fatality function This function models the coupling between the shortage of health care resources and the fatality rate δ_D at hospitals. Denote the transition rates from hospitalized to recovered and to dead as a function of the fatality rate δ_D, namely, $\gamma_{HR} = (1-\delta_D)/\tau_h$ and $\gamma_{HD} = \delta_D/\tau_h$. We define δ_{D0} as the base fatality rate of hospitalized individuals in the condition of supply sufficiency. δ_{D1} measures the increment of the fatality rate under the shortage of critical medical supplies. Under this assumption, we model the fatality rates as a time-evolving parameter depending on the shortage in health care and medical supply as

$$\delta_D(t) = \delta_{D0} + c_h(t)\delta_{D1}, \tag{13}$$

where c_h is zero when medical supplies are sufficient, and is 1 in the real-world scenario when the severe shortage of medical supplies is experienced. All parameters are calculated directly from real-world data or from parameter fitting unless specified.

Parameter Fitting

We use the data reported by Johns Hopkins University Center[30] from January 22, 2020 to September 24, 2020 as our dataset for model fitting. The data provides time-series of daily updates on the new infected cases, fatalities and recovered cases. The objective is to identify the parameters of the compartmental model in such a way that the simulated data matches the data as much as possible. The simulated data are obtained by numerically solving the model in Eqs. (1) - (6) using an integration algorithm.

A two-step fitting process is performed to obtain the best parameters for the system of coupled disease dynamics consisting of six regions. In the first step, we considered the disease in each region independently without considering the cross-coupling terms ($\beta_{ij}, i \neq j$) in the dynamics. To accomplish the parameter identification, we solved a nonlinear constrained least-squares problem for each region to minimize the cost function between the model prediction and the data. We devised the cost function based on a sum of the mean square error for daily infected and fatalities. We did not include the recovered individuals in the cost function since the definition of recovery in the equations (i.e., not infectious) and those reported in data (i.e., cured) might not be consistent. The initial number of infected and recovered cases for the SEIHRD model was considered as the data. Also, due to lack of information regarding the initial number of exposed individuals (E_0), it was assumed to be five times of the initial number of infected individuals. To capture rapidly changing social scenarios particularly during the initial period of the COVID-19 spread, we split the integration interval into sub-intervals of 20 days, and the best parameters ($\beta_i, \delta_{Hi}, \delta_{Di}$) were found at each sub-interval (the parameters are assumed to be constant in each sub-interval).

Next, we use the fitted parameters as an initial guess to fit the coupled equations (1) and (2) simultaneously for all regions considering the cross-coupling terms. The disease in each region is connected to that of other regions by the cross-transmission

terms, $\beta_{i,j}, i \neq j$. To identify the best parameters for the coupled system, we fix the values of c_i and d_i to the levels identified in the decoupled fitting, and search for the best transmission matrix G that fits the data. We define the transmission matrix G as $G_{i,j}(t) = \varepsilon p_{i,j}(t)\beta_i(t), i \neq j$, $G_{i,j}(t) = \beta_i(t), i = j$, where $p_{i,j}$ is a coefficient proportional to the number of daily travels from region j to region i adjusted by the change in the international air travels reported by International Air Transport Association (IATA) since starting the pandemic [48], and ε is a fixed small number ($\varepsilon \ll 1$) reflecting that cross-coupling has considerably smaller effect on the disease transmission compared to the internal transmission. During each sub-interval, we seek for the best β_i and also the best ε that fit the worldwide COVID-19 data. It is observed that the suggested model and parameter estimation approach fit the data with a reasonable accuracy. The trend of optimal tuning of the model parameters for each region is shown in Fig. 7.

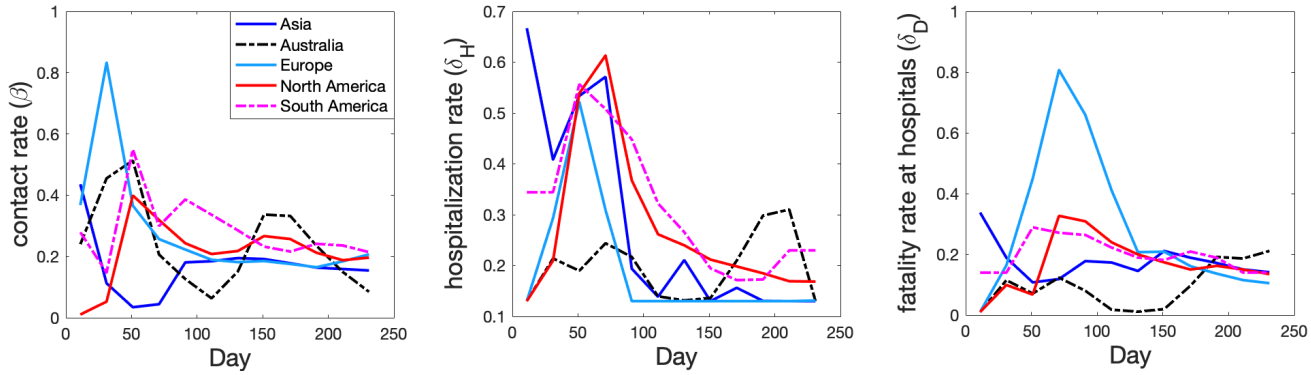

Figure 7. Disease dynamics coefficients obtained by fitting the coupled equations to COVID-19 data starting from January 22, 2020 to September 24, 2020

Network proactive control

It is important to foresee the impact of managerial decisions on the trend of supply chain disruption to proactively create an agile and time-sensitive containment strategy. Due to the nonlinearity in the disease dynamics and in the coupling function, linear approximation is conducted following the first order terms of Taylor series expansion assuming a given initial condition in the planning horizon. Systems are updated in each time point to enforce the accuracy of the approximation. For a specific time point t, the forecast of future disease dynamics, Eq. (1) - (6), of time τ follows

$$S_i(\tau+1) = \mu_0 + (1+\mu_1^i)S_i(\tau) + \sum_j \mu_2^{i,j} I_j(\tau) + \sum_j \mu_3^{i,j} U_{j,k}(\tau) + \varepsilon_1^i \quad (14)$$

$$E_i(\tau+1) = -\mu_0 - \mu_1^i S_i(\tau) - \sum_j \mu_2^{i,j} I_j(\tau) - \sum_j \mu_3^{i,j} U_{j,k}(\tau) + (1-\gamma_{EI})E_i(\tau) - \varepsilon_1^i \quad (15)$$

$$I_i(\tau+1) = I_i(t) + \gamma_{EI} E_i(t) - (\gamma_{IH} + \gamma_{IR}) I_i(t) \quad (16)$$

$$H_i(\tau+1) = H_i(\tau) + \gamma_{IH} I_i(\tau) - \tau_H H_i(\tau) \quad (17)$$

$$R_i(\tau+1) = R_i(\tau) + \gamma_{IR} I_i(\tau) + \gamma_{HR}(t) H_i(\tau) + \mu_4^i U_{i,h}(\tau) + \varepsilon_2^i \quad (18)$$

$$D_i(\tau+1) = D_i(\tau) + \gamma_{HD}(t) H_i(\tau) - \mu_4^i U_{i,h}(\tau) - \varepsilon_2^i \quad (19)$$

where

$$\mu_1^i = \left.\frac{\partial S_i(t+1)}{\partial S_i}\right|_{S_i(t),E_i(t),U_{i,h}(t),I_j(t)} = -\sum_j \frac{\beta_{i,j}(\theta^j(t),U_{i,h}(t))I_j(t)}{N_j} \tag{20}$$

$$\mu_2^{i,j} = \left.\frac{\partial S_i(t+1)}{\partial I_j}\right|_{S_i(t),E_i(t),U_{i,h}(t),I_j(t)} = -\frac{\beta_{i,j}(\theta^j(t),U_{i,h}(t))S_j(t)}{N_j} \tag{21}$$

$$\mu_3^{i,j} = \left.\frac{\partial S_i(t+1)}{\partial U_{i,h}(t)}\right|_{S_i(t),E_i(t),U_{i,h}(t),I_j(t)} = \frac{2S_i(t)I_j(t)c_{N,i}(t)\beta_0(P_l-1)}{N_j(P_l+1)} \frac{\frac{10^6}{N_i}e^{\frac{10^6}{N_i}U_{j,h}(t)}}{(1+e^{\frac{10^6}{N_i}U_{j,h}(t)})^2} \tag{22}$$

$$\mu_4^i = \left.\frac{\partial R_i(t+1)}{\partial U_{i,h}(t)}\right|_{S_i(t),E_i(t),U_{i,h}(t),I_j(t)} = H_i(t)\tau_H\delta_{D1}\frac{2(P_l-1)}{(1+P_l)} \frac{\frac{10^6}{N_i}e^{\frac{10^6}{N_i}U_{i,h}(t)}}{(1+e^{\frac{10^6}{N_i}U_{i,h}(t)})^2} \tag{23}$$

$$\varepsilon_1^i = -[\mu_1^i,\mu_2^{i,j},\mu_3^{i,j}]\begin{bmatrix} S_i(t) \\ I_j(t) \\ U_{j,h}(t) \end{bmatrix} \tag{24}$$

$$\varepsilon_2^i = -\mu_4^i U_{i,h}(t) \tag{25}$$

The disease-dependent capacity function in Eq. (9) is also linearized to obtain

$$w_{i,k}(\tau) \le -\frac{e^{-\frac{\gamma_w I_i(t)}{N_i}}}{N_i} I_i(\tau) + \left(1+\frac{\gamma_w I_i(t)}{N_i}\right) e^{-\frac{\gamma_w I_i(t)}{N_i}} \bar{W}_{i,k} \tag{26}$$

With coupled dynamic systems there is no action that is exerted into the disease directly, but the changes in the supply chain propagate to the disease dynamics by affecting the remaining demands of HHS resources, $U_{i,h}(t)$ in Eqs. (14),(15),(18),(19). The coupled network analysis enables managerial decisions aware of changes in both the disease dynamics and the supply chain as well as the opportunity to trade-off the objectives in disease growth and economic losses. The containment strategy is formulated by the following mathematical model, aiming to minimize the total fatalities, economic losses, and managerial cost

$$\begin{aligned}
\min_{o_{i,i',k},w_{i,k},o_{i,k}} \quad & D(t+t_p) + c_u \sum_{\tau=t+1}^{\tau=t+t_p} \sum_k \sum_i U_{i,k}(\tau) + c_p w_{i,k} + \sum_{i'\neq i} c_l o_{i,i',k} \in [t,t+t_p] \\
\text{s.t.} \quad & (a)\ o_{i,i',k}(\tau), w_{i,k}(\tau), o_{i,k}(\tau) \ge 0, \quad \forall i,i',k,\tau \\
& (b)\ V_{i,k}(\tau), U_{i,k}(\tau) \ge 0, \quad \forall i,k,\tau \in [t,t+t_p] \\
& (c)\ w_{i,k}(\tau) \le -\frac{e^{-\frac{\gamma_w I_i(t)}{N_i}}}{N_i} I_i(\tau) + (1+\frac{\gamma_w I_i(t)}{N_i}) e^{-\frac{\gamma_w I_i(t)}{N_i}} \bar{W}_{i,k}, \quad \forall i,k,\tau \in [t,t+t_p] \\
& (d)\ V_{i,k}(\tau) \le \bar{V}_{i,k}, \quad \forall i,k,\tau \in [t,t+t_p]
\end{aligned} \tag{27}$$

where t_p is the planning horizon, which is 14 days in this study, c_u is the weight of the total economic losses compared to the total fatalities in the planning horizon, $c_{p,k}$ and $c_{l,k}$ are the production cost and trade cost to obtain a resource of type k, where $c_{p,k} < c_{l,k}$, $\bar{V}_{i,k}$ and $\bar{W}_{i,k}$ specify the maximum production capacity and inventory capacity. Constraint (a) ensures that

all supply chain management decisions are non-negative; (b) indicates that the amount of inventory stocks are non-negative; (c) ensures that production decisions of a certain area are always constrained by the available capacity $\bar{W}$; (d) ensures that the inventory stocks are constrained by a regional inventory threshold $\bar{V}$. The model is solved by the *Cplex* package[49]. The managerial decisions are imported to the coupled network model described by Eqns.(1) to (8) to simulate the changes in the demand, inventory and disease. The coupled model and managerial decisions are updated at each time point (i.e., daily) to achieve a time-sensitive containment strategy.

References

1. Rothan, H. A. & Byrareddy, S. N. The epidemiology and pathogenesis of coronavirus disease (COVID-19) outbreak. *J. autoimmunity* 102433 (2020).

2. Ivanov, D. & Das, A. Coronavirus (COVID-19/SARS-CoV-2) and supply chain resilience: A research note. *Int. J. Integr. Supply Manag.* **13**, 90–102 (2020).

3. Ivanov, D. & Dolgui, A. Viability of intertwined supply networks: extending the supply chain resilience angles towards survivability: A position paper motivated by COVID-19 outbreak. *Int. J. Prod. Res.* **58**, 2904–2915 (2020).

4. Azevêdo, D. Trade set to plunge as COVID-19 pandemic upends global economy. In *WTO Trade Forecast Press Conference*, vol. 8 (2020).

5. Cook, T. Personal protective equipment during the coronavirus disease (COVID) 2019 pandemic–a narrative review. *Anaesthesia* (2020).

6. Chughtai, A. A., Seale, H. & Macintyre, C. R. Effectiveness of cloth masks for protection against severe acute respiratory syndrome coronavirus 2. *Emerg. infectious diseases* **26** (2020).

7. Derraik, J. G., Anderson, W. A., Connelly, E. A. & Anderson, Y. C. Rapid review of SARS-CoV-1 and SARS-CoV-2 viability, susceptibility to treatment, and the disinfection and reuse of PPE, particularly filtering facepiece respirators. *Int. journal environmental research public health* **17**, 6117 (2020).

8. Arafat, S. Y. *et al.* Panic buying: An insight from the content analysis of media reports during COVID-19 pandemic. *Neurol. Psychiatry Brain Res.* **37**, 100–103 (2020).

9. Paul, S. K. & Chowdhury, P. A production recovery plan in manufacturing supply chains for a high-demand item during COVID-19. *Int. J. Phys. Distribution & Logist. Manag.* (2020).

10. Siddiqui, F. The US forced major manufacturers to build ventilators. now they're piling up unused in a strategic reserve (2020).

11. Ranney, M. L., Griffeth, V. & Jha, A. K. Critical supply shortages—the need for ventilators and personal protective equipment during the COVID-19 pandemic. *New Engl. J. Medicine* **382**, e41 (2020).

12. Dai, T., Bai, G. & Anderson, G. F. PPE supply chain needs data transparency and stress testing. *J. general internal medicine* 1–2 (2020).

13. Swaminathan, A. *et al.* Personal protective equipment and antiviral drug use during hospitalization for suspected avian or pandemic influenza1. *Emerg. infectious diseases* **13**, 1541 (2007).

14. Bradsher, K. & Alderman, L. The world needs masks. China makes them—but has been hoarding them. *New York Times* **13** (2020).

15. Alderman, L. As coronavirus spreads, face mask makers go into overdrive. *New York Times* **8** (2020).

16. Furman, E. *et al.* Prediction of personal protective equipment use in hospitals during COVID-19. *arXiv preprint arXiv:2011.03002* (2020).

17. World Health Organization. Coronavirus disease (COVID-19) advice for the public: when and how to use masks (2020).

18. Sforza, A. & Steininger, M. Globalization in the time of COVID-19. (2020).

19. Whitworth, J. COVID-19: a fast evolving pandemic. *Transactions The Royal Soc. Trop. Medicine Hyg.* **114**, 241 (2020).

20. Alvarez, F. E., Argente, D. & Lippi, F. A simple planning problem for COVID-19 lockdown. Tech. Rep., National Bureau of Economic Research (2020).

21. Zhang, J. *et al.* Investigating time, strength, and duration of measures in controlling the spread of COVID-19 using a networked meta-population model. *Nonlinear Dyn.* 1–12 (2020).

22. Li, T., Liu, Y., Li, M., Qian, X. & Dai, S. Y. Mask or no mask for COVID-19: A public health and market study. *PloS one* **15** (2020).

23. Cohen, J. & van der Meulen Rodgers, Y. Contributing factors to personal protective equipment shortages during the COVID-19 pandemic. *Prev. Medicine* 106263 (2020).

24. World Health Organization and others. Rational use of personal protective equipment for coronavirus disease (COVID-19): interim guidance. Tech. Rep., World Health Organization (2020).

25. MacIntyre, C. R. *et al.* Efficacy of face masks and respirators in preventing upper respiratory tract bacterial colonization and co-infection in hospital healthcare workers. *Prev. medicine* **62**, 1–7 (2014).

26. McGarry, B. E., Grabowski, D. C. & Barnett, M. L. Severe staffing and personal protective equipment shortages faced by nursing homes during the COVID-19 pandemic: Study examines staffing and personal protective equipment shortages faced by nursing homes during the COVID-19 pandemic. *Heal. Aff.* 10–1377 (2020).

27. Lockhart, S. L., Duggan, L. V., Wax, R. S., Saad, S. & Grocott, H. P. Personal protective equipment (PPE) for both anesthesiologists and other airway managers: principles and practice during the COVID-19 pandemic. *Can. J. Anesth. canadien d'anesthésie* 1–11 (2020).

399 **28.** White, D. B. & Lo, B. A framework for rationing ventilators and critical care beds during the COVID-19 pandemic. *Jama*
400 **323**, 1773–1774 (2020).

401 **29.** Pearce, J. M. A review of open source ventilators for COVID-19 and future pandemics. *F1000Research* **9** (2020).

402 **30.** Dong, E., Du, H. & Gardner, L. An interactive web-based dashboard to track COVID-19 in real time. *The Lancet infectious*
403 *diseases* **20**, 533–534 (2020).

404 **31.** China: Country-specific: Arrivals of non-resident visitors at national borders, by nationality 2014 - 2018 (12.2019).
405 *Tour. Stat.* null, DOI: 10.5555/unwtotfb0156012120142018201912 (2020). https://www.e-unwto.org/doi/pdf/10.5555/
406 unwtotfb0156012120142018201912.

407 **32.** Andrew, R. M. & Peters, G. P. A multi-region input–output table based on the global trade analysis project database
408 (GTAP-MRIO). *Econ. Syst. Res.* **25**, 99–121 (2013).

409 **33.** ONS. UK standard industrial classification of economic activities 2007 (SIC 2007) structure and explanatory notes (2009).

410 **34.** HSE. Human health and social work activities statistics in great britain 2020 (2020).

411 **35.** Yu, X., Liu, C., Wang, H. & Feil, J.-H. The impact of COVID-19 on food prices in China: evidence of four major food
412 products from beijing, shandong and hubei provinces. *China Agric. Econ. Rev.* (2020).

413 **36.** Polansek, P. K., Tom. Coronavirus disrupts china meat imports, food supply during pork shortage. *Reuters* (2020).

414 **37.** Vardavas, R. *et al.* The health and economic impacts of nonpharmaceutical interventions to address COVID-19. (2020).

415 **38.** Guan, D. *et al.* Global supply-chain effects of COVID-19 control measures. *Nat. Hum. Behav.* 1–11 (2020).

416 **39.** Wynants, L. *et al.* Prediction models for diagnosis and prognosis of COVID-19: systematic review and critical appraisal.
417 *bmj* **369** (2020).

418 **40.** Li, L. *et al.* Propagation analysis and prediction of the COVID-19. *Infect. Dis. Model.* **5**, 282–292 (2020).

419 **41.** Newton, P. N. *et al.* COVID-19 and risks to the supply and quality of tests, drugs, and vaccines. *The Lancet Glob. Heal.* **8**,
420 e754–e755 (2020).

421 **42.** Lorenz, E. N. Deterministic nonperiodic flow. *J. atmospheric sciences* **20**, 130–141 (1963).

422 **43.** Keeling, M. J. & Rohani, P. *Modeling infectious diseases in humans and animals* (Princeton University Press, 2011).

423 **44.** Moghadas, S. M. *et al.* Projecting hospital utilization during the COVID-19 outbreaks in the united states. *Proc. Natl.*
424 *Acad. Sci.* **117**, 9122–9126 (2020).

425 **45.** Feng, S. *et al.* Rational use of face masks in the COVID-19 pandemic. *The Lancet Respir. Medicine* **8**, 434–436 (2020).

426 **46.** Li, T., Liu, Y., Li, M., Qian, X. & Dai, S. Y. Mask or no mask for COVID-19: A public health and market study. *PloS one*
427 **15**, e0237691 (2020).

428 **47.** Jung, H. *et al.* Comparison of filtration efficiency and pressure drop in anti-yellow sand masks, quarantine masks, medical
429 masks, general masks, and handkerchiefs. *Aerosol Air Qual. Res.* **14**, 991–1002 (2013).

430 **48.** International Air Transport Association and others. Air passenger market analysis. *Montreal: Int. Air Transp. Assoc.*
431 (2014).

432 **49.** CPLEX, IBM ILOG. V12. 1: User's manual for CPLEX. *Int. Bus. Mach. Corp.* **46**, 157 (2009).

433 Author contributions

434 X.L., A.G., and B.I.E. designed the study and developed the algorithm. X.L. and A.G. contributed equally to developing
435 coupling functions and performing the numerical simulations with input from B.I.E. X.L. formulated the supply chain network
436 and developed the network proactive control. A.G. formulated the disease model and conducted parameter fitting. J.D. and P.R.
437 provided feedback in model formulation and data interpretation. X.L. and A.G. analyzed results and wrote the initial draft with
438 help from all authors. All authors reviewed and approved the manuscript. B.I.E. supervised the project.

439 Competing Interests

440 The authors declare no competing interests.

441 Additional information

442 **Reprints and permissions information** is available at www.nature.com/reprints.

443 **Correspondence and requests for materials** should be addressed to B.I.E.

444 **Publisher's note** Springer Nature remains neutral with regard to jurisdictional claims in published maps and institutional
445 affiliations.

447 Data availability

448 **Global trade dataset.**The global trade dataset used to stimulate the presented results are licensed by the Global Trade Analysis
449 Project at the Center for Global Trade Analysis in Purdue University's Department of Agricultural Economics. The analyses
450 performed in this paper are based on version 10 of the dataset. Due to the restriction in the licensing agreement with GTAP, the
451 authors have no right to disclose the original dataset publicly.

452 **COVID-19 dataset.** We use the data reported by Johns Hopkins University Center as our dataset for model fitting. All data
453 and methods needed to reproduce the results in the paper are provided in the paper or as supplementary materials. This dataset
454 is publicly available at (https://raw.githubusercontent.com/datasets/covid-19/master/data/countries-aggregated.csv)

Code availability

The code will be available upon the request

Figures

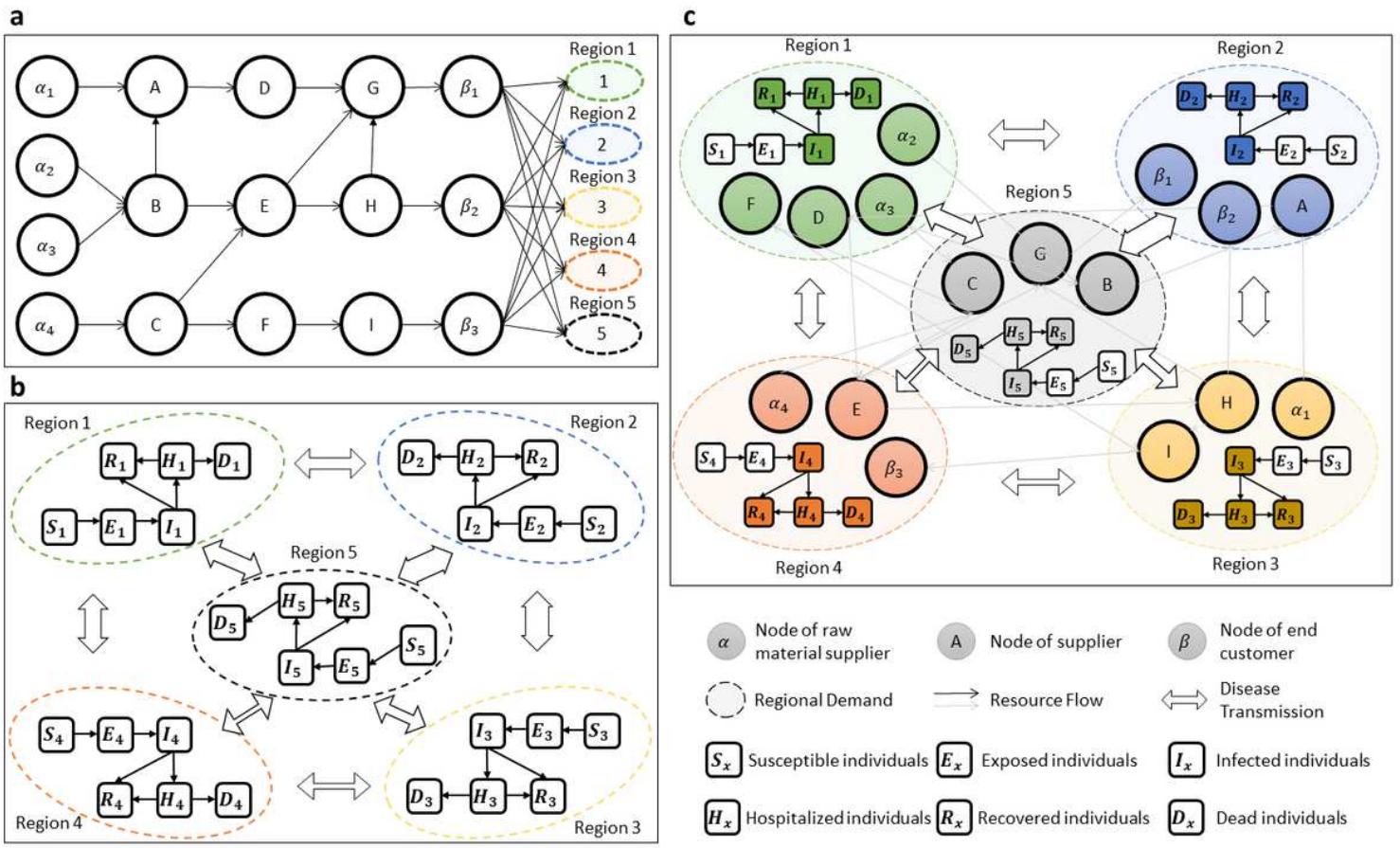

Figure 1

System Model of supply chain and disease dynamic: a) a classic supply chain network with three types of products; b) a classic multi-patch disease network for COVID-19; c) the coupled networks of multi-patch disease and the production and supply chain.

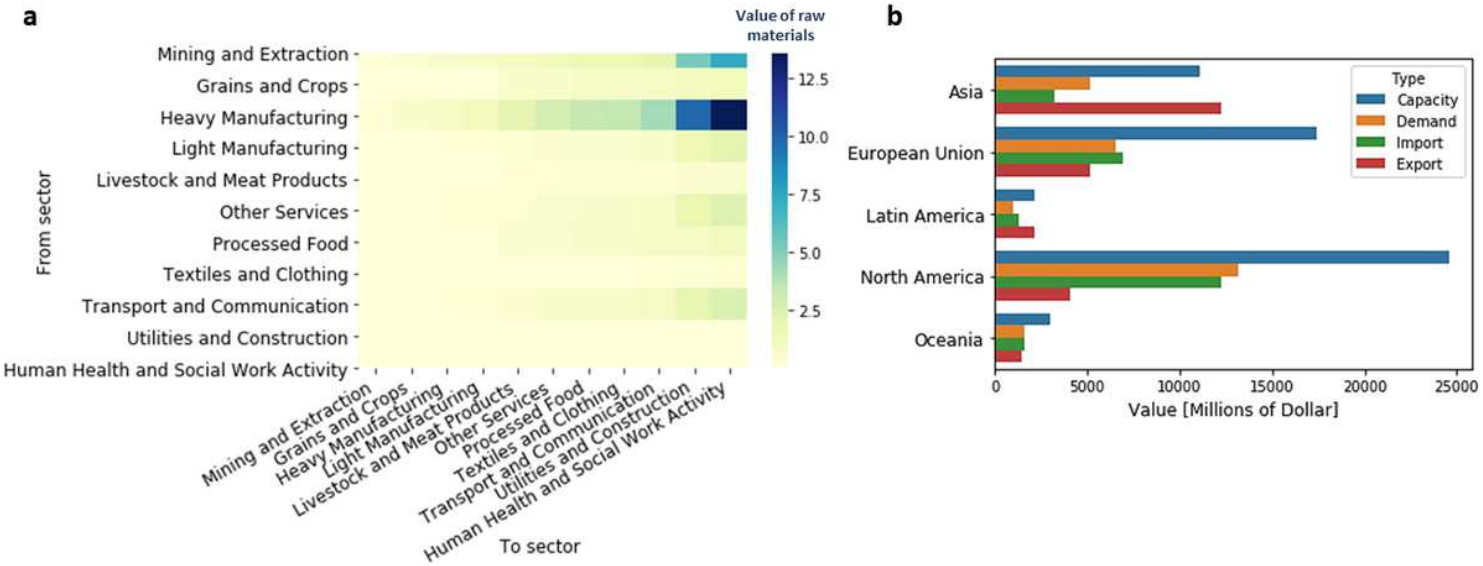

Figure 2

Global trade data analysis based on GTAP 10: a) Values of required raw material from different sectors to satisfy the doubled production of each sector. The rows of the table define sectors to provide the raw materials, and the columns of the table define sectors which double their production. b) Comparison of the production capacity, demands, and trade at the equilibrium between different regions. Here, the capacity is calculated by the total yearly production estimated from the total export and self-consumed resources. Demands are estimated based on the resource consumption from the household and government. Trade history is calculated based on resources exchanges in each region, including household, government, and companies.

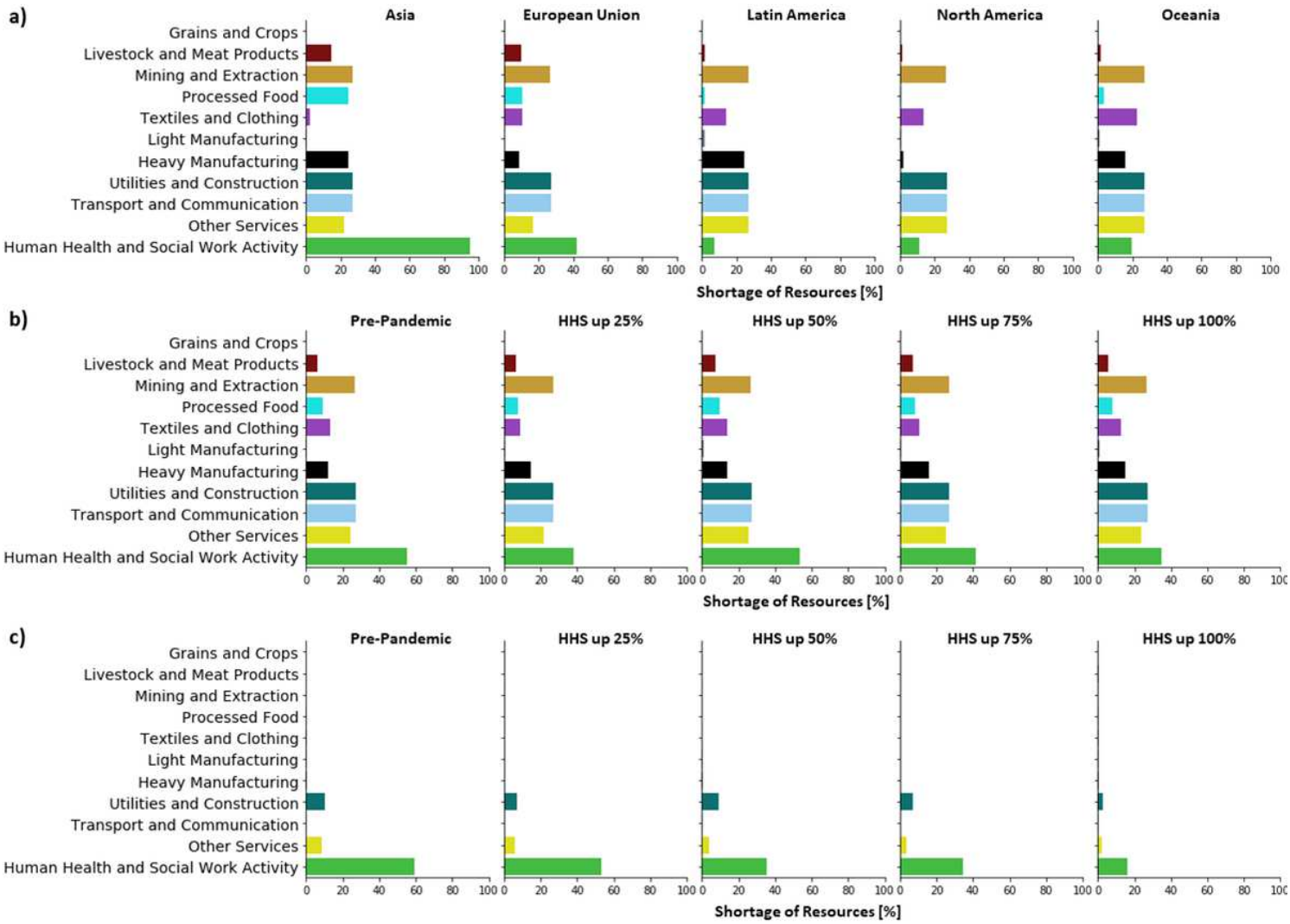

Figure 3

Sectoral impacts of increased HHS capacity: a) Without coordinating other sectors, the regional shortage of resources after doubling the production of HHS in each region. b) Without coordinating other sectors, the averaged shortage of resource in five ramp-up scenarios, in terms of the pre-pandemic capacity (100), ramp-up by 25% (125), ramp-up by 50% (150), ramp-up by 75% (175) and , ramp-up by 100% (200). c) With coordinated supply chains, the averaged shortage of resource in five production ramp-up scenarios.

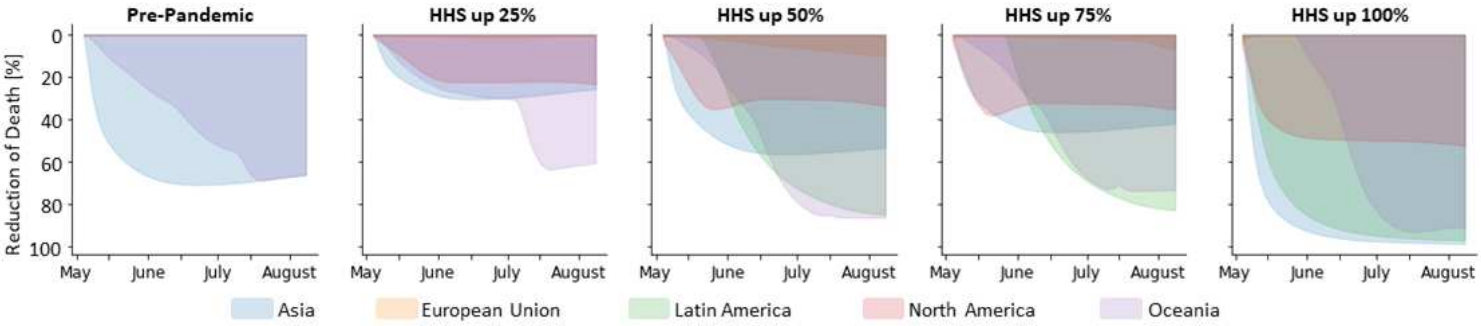

Figure 4

Disease impacts for increased HHS capacity. Assuming coordination of the supply chain is possible, the diagrams show the perentage of fatality reduction in different regions with the increasing production capacity of HHS resources, in terms of the pre-pandemic capacity (100), ramp-up by 25% (125), ramp-up by 50% (150), ramp-up by 75% (175) and , ramp-up by 100% (200). The fatalities simulated in the pre-pandemic capacities is used as a benchmark to calculate the reduction percentage.

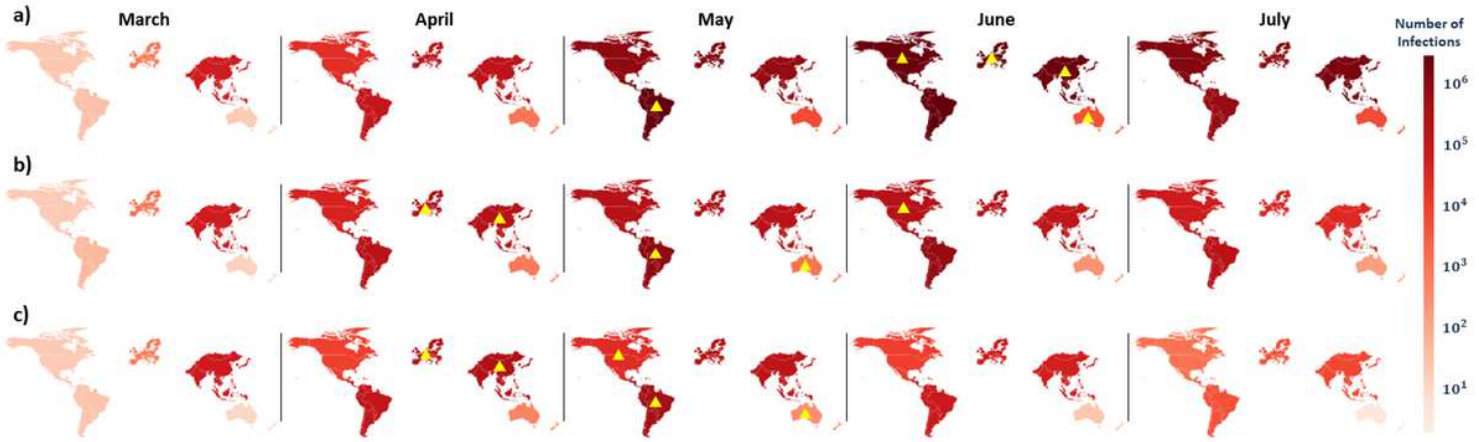

Figure 5

Impacts of strategies on infections: a) The evolving infections under the pre-pandemic containment strategy. b) The evolving infections for the SCO strategy. c) The evolving infections for the CNO strategy. The darkness of each region represents the number of infections. The yellow triangle marks the occurrence of the peak of infection. Note: The designations employed and the presentation of the material on this map do not imply the expression of any opinion whatsoever on the part of Research Square concerning the legal status of any country, territory, city or area or of its authorities, or concerning the delimitation of its frontiers or boundaries. This map has been provided by the authors.

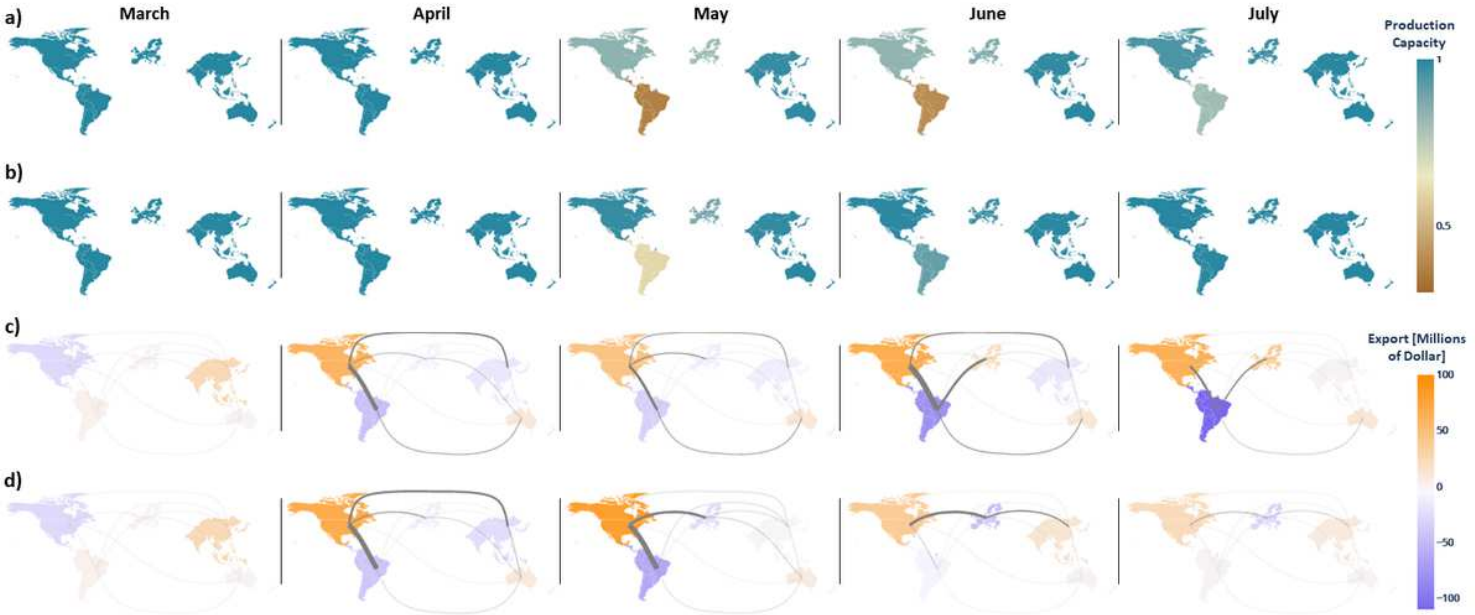

Figure 6

Production disruption and trade decisions of different containment strategies: a) The dynamics of available production capacity by region in the SCO strategy. The color bar represents the percentage of available production capacity of each region. b) The dynamics of available production capacity in the CNO scenario. c) The total import and export decisions of each month in the SCO strategy; The strength of connections of regions marked by the width of the corresponding lines. d) The total import and export decisions of each month in the CNO strategy; the strength of connections of regions marked by the width of the corresponding lines. Note: The designations employed and the presentation of the material on this map do not imply the expression of any opinion whatsoever on the part of Research Square concerning the legal status of any country, territory, city or area or of its authorities, or concerning the delimitation of its frontiers or boundaries. This map has been provided by the authors.

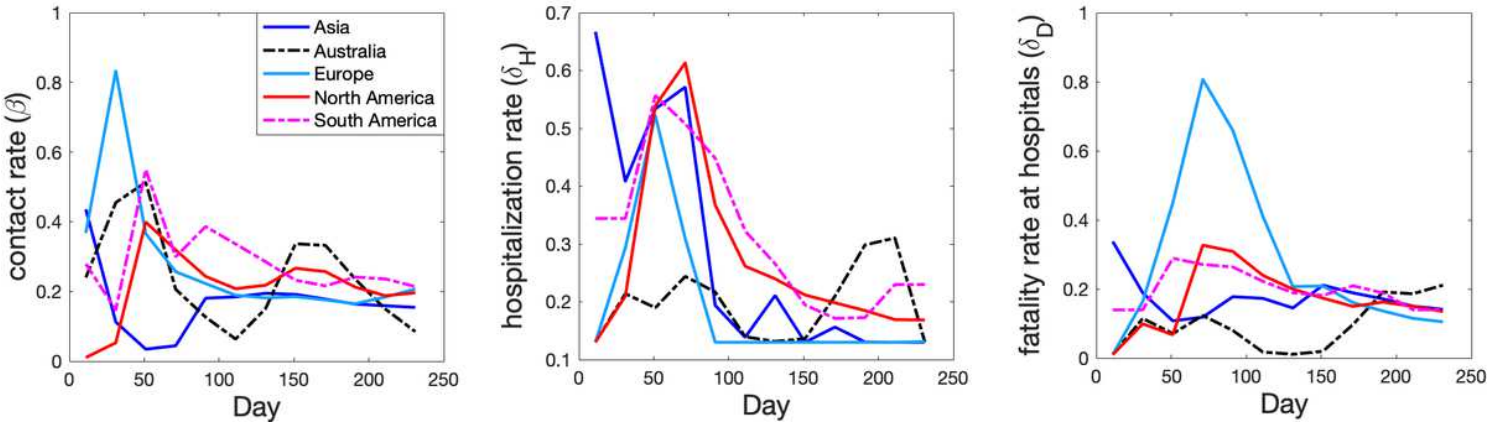

Figure 7

Disease dynamics coefficients obtained by fitting the coupled equations to COVID-19 data starting from January 22, 2020 to September 24, 2020